Fuel 383 (2025) 133750

Contents lists available at ScienceDirect

Fuel

journal homepage: www.elsevier.com/locate/fuel

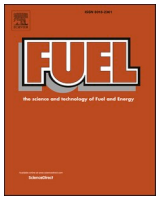

Full Length Article

Polycyclic aromatic hydrocarbons formed during the pyrolysis of dimethoxymethane (DMM). Comparison with other oxygenated additives

Fausto Viteri *, Katiuska Alexandrino, Ángela Millera, Rafael Bilbao, María U. Alzueta *

Aragón Institute of Engineering Research (I3A), Department of Chemical and Environmental Engineering, University of Zaragoza, Río Ebro Campus 50018, Zaragoza, Spain

ARTICLE INFO

Keywords:
Dimethoxymethane
Oxygenates
Pyrolysis
PAH
B[*a*]P
Soot

ABSTRACT

The influence of the temperature (1075 – 1475 K) and inlet concentration of fuel (33,333 and 50,000 ppmv) on the formation of the 16 EPA-priority Polycyclic Aromatic Hydrocarbons (PAH) from the pyrolysis of dimethoxymethane (DMM) was analyzed. PAH were detected in different phases (gas phase, adsorbed on soot, and stuck on the reactor walls) and quantified by gas chromatography-mass spectrometry (GC–MS). Additionally, the toxicity of the PAH samples, expressed as B[*a*]P-eq, was analyzed in all experiments. A comparison with the results obtained from the pyrolysis of other oxygenated compounds was also performed and similar behaviors were observed. The main results showed that, at low temperatures, the highest concentrations of PAH were found in the gas phase, while at high temperatures were found on soot. For both inlet concentrations of DMM, the light PAH, such as naphthalene and acenaphthylene, were found in major concentrations, in all phases and temperatures. The heavy PAH, such as fluoranthene and pyrene, increased its concentration on soot at highest temperatures. The highest formation of soot was obtained at 1475 K and follows the trend: 2,5DMF < *tert*-butanol < 2MF < 2butanol < *iso*-butanol < 1-butanol < ethanol < DMC < DMM. The highest formation of PAH was at 1275 K with the tendency: *tert*-butanol < 2-butanol < 1-butanol < 2,5DMF < 2MF < *iso*-butanol < ethanol < DMC < DMM. The highest B[*a*]P-eq value was found in the pyrolysis of 2,5DMF, and the lowest in the pyrolysis of DMM.

1. Introduction

The continuous impact on the climate by atmospheric emission sources has led to the search for alternatives to fossil fuels in recent years. Within this framework, the biorefinery has set different compounds that contribute to improving the combustion process as they provide a high amount of oxygen and characteristics that give them better performance at the level of internal combustion engines, especially in the automotive industry. Among those, different oxygenated compounds have been considered due to their chemical and mechanical characteristics, such as octane and cetane numbers, heating value, etc.

Previous research has shown that different oxygenated compounds can effectively reduce diesel engine emissions, mainly particulate matter (PM). Specifically, compounds belonging to the Oxymethylene Dimethyl Ethers (OME_x) group, which are synthetic acyclic ether fuels with the chemical structure $CH_3O(CH_2O)_nCH_3$ (n = 0–5), have gained great interest due to their high cetane number, high oxygen content, and the absence of C–C bonds which promote negligible soot emissions [1].

Dimethoxymethane (DMM, $CH_3OCH_2OCH_3$) is part of this group of compounds, with a high cetane number [2] and a high oxygen content by weight (42 %). Even DMM could be a better option for diesel/oxygenate blends than the OME_0 ultra-clean-burning, dimethyl ether (DME, CH_3OCH_3), due to its higher solubility with diesel fuel, lower vapor pressure, higher cetane number, and higher quantity of oxygen [3].

Different studies have been performed using diesel/DMM blends to evaluate the engine performance and emissions. For example, Sathiyagnanam et al. [4] blended DMM with diesel in a single cylinder direct injection (DI) diesel engine and observed an appreciable reduction of emissions, smoke density, PM and an increase in the engine performance, when compared with a normal diesel run. Zhu et al. [5] investigated combustion characteristics, fuel efficiency and emissions of a compression-ignition engine fueled with DMM blends. They found that the thermal efficiency was improved and that the DMM presence was beneficial for the reduction of smoke and CO emissions, as well as particulate matter. Pan et al. [6] studied the effect of diesel/DMM blends on

* Corresponding authors.
E-mail addresses: fviteri@unizar.es (F. Viteri), uxue@unizar.es (M.U. Alzueta).

https://doi.org/10.1016/j.fuel.2024.133750
Received 13 June 2024; Received in revised form 7 October 2024; Accepted 12 November 2024
Available online 27 November 2024

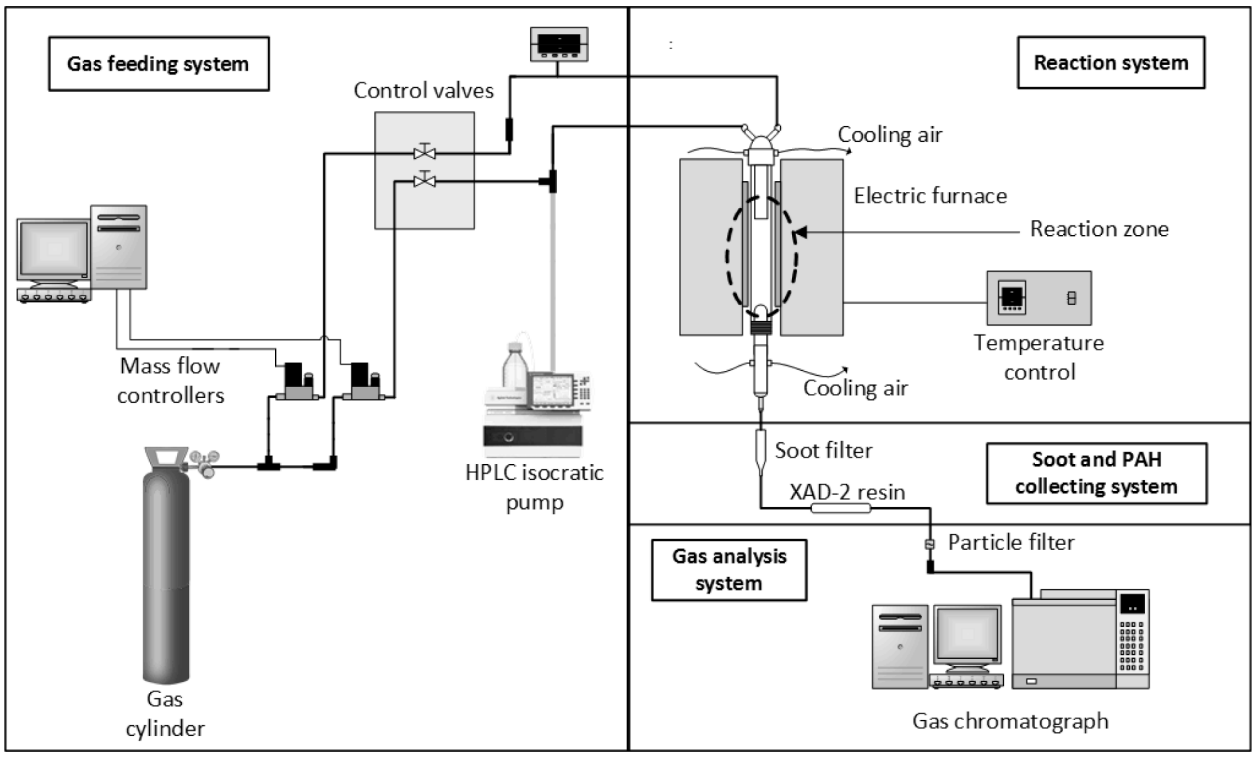

Fig. 1. Experimental setup: gas feeding, reaction, collection of soot and PAH, and gas analysis systems.

the combustion and emission characteristics in a four-cylinder commercial compression ignition (CI) engine and the results indicated that the addition of DMM improves the brake thermal efficiency of diesel engine and significantly reduce soot emissions. Due to the contribution of DMM on decreasing PM emissions in CI engines, different experiments have been carried out in flames [7–10], jet-stirred reactors [11–15], flow reactors [16–19], shock tubes [11,19–23], rapid compression machines [8,19], in conjunction with detailed chemical kinetic modeling to acquire an in-depth knowledge of DMM chemical conversion.

The efforts to understand the conversion of DMM have focused mainly on its oxidation, while pyrolysis studies are still scarce. The studies on the pyrolysis of DMM have been carried out mainly to obtain the concentration of light hydrocarbons produced and to analyze the reaction kinetics of DMM conversion e.g. [8,9]. However, few efforts have been made to study other aspects of the DMM pyrolysis, such as formation of soot and Polycyclic Aromatic Hydrocarbons (PAH) [24]. In our previous work [25], the DMM pyrolysis was investigated in a plug flow reactor operating at atmospheric pressure, in the temperature range of 1075–1475 K and with inlet concentrations of fuel of 33,333 and 50,000 ppmv. That work focused on the gas-phase analysis (C_2H_2, C_2H_4, C_6H_6, H_2, CH_4, CO and CO_2) and the soot formation, together with the development of a gas-phase model to describe the process. Moreover, the interaction of the soot formed with O_2 and with NO, and soot characterization (elemental analysis, physical adsorption with N_2, Transmission Electron Microscopy (TEM), X-Ray Diffraction (XRD) and Raman spectroscopy) were investigated. In this way, the present work complements the previous study by reporting the concentration of the 16 EPA-priority PAH obtained during the pyrolysis of DMM.

PAH are a large group of organic compounds containing three or more fused aromatic rings originated by natural (e.g. forest fires, volcanoes) and anthropogenic (e.g. burning of fossil fuels during heating processes, waste incinerators, automobile exhausts) sources [26], being their formation favored under high temperatures, fuel-rich and pyrolytic conditions. These compounds are known to be hazardous to human health, mainly the 16 PAH classified by the United States Environmental Protection Agency (U.S. EPA) as priority pollutants (EPA - PAH) [27], i.e., naphthalene (NAPH), acenaphthylene (ACNY), acenaphthene (ACN), fluorene (FLUO), phenanthrene (PHEN), anthracene (ANTH), fluoranthene (FANTH), pyrene (PYR), benzo(*a*)anthracene (B[*a*]A), chrysene (CHR), benzo(*b*)fluoranthene (B[*b*]F), benzo(*k*)fluoranthene (B[*k*]F), benzo(*a*)pyrene (B[*a*]P), indene[123-*cd*]pyrene (I[123-*cd*]P), dibenzo(*ah*)anthracene (DB[*ah*]A) and benzo[*g,h,i*]perylene (B[*ghi*]P). B[*a*]P is used as a reference compound to assess the health risk associated with exposure to PAH [28,29].

PAH are important intermediates in the soot formation process, which is not yet fully defined due to its complexity. However, it is well accepted that the soot formation process starts with the formation of linear hydrocarbons, such as C_2H_2, C_3H_x, C_4H_x, etc., to produce the first aromatic ring, which is generally benzene. The, aromatic rings and other hydrocarbon intermediate species gradually grow into PAH. There are different mechanisms proposed to explain the formation of PAH, such as the hydrogen abstraction-acetylene addition (HACA) [30], the combinative growth, such as propargyl radical recombination, [31,32], and the Diels - Alder [33] mechanisms, all them may be present in a PAH and soot formation scenario. Once formed, subsequently PAH react among them to form nascent soot (known as particle inception), and then gas-phase molecules, such as acetylene and PAH, react on the surface of growing particles [34,35]. Immediately, particle coagulation occurs through the collision of growing soot particles, producing new spherical structures [36], which agglomerate into irregular units, i.e., forming chain-like structures [37].

In addition to the PAH being involved in the soot formation process, they can also appear adsorbed on the soot surface which increase the human health risk of these particles. In this way, PAH can be distributed in different phases (soot, air) depending upon their molecular weight, vapor pressure, temperature, pressure, concentration of PAH and soot characteristics [38,39].

As DMM is proposed as a fuel additive, it is important not only to study soot formation but also PAH formation during its conversion, which can be affected by operating conditions, such as temperature or concentration of fuel and, to our knowledge, it has not been studied so far. In this way, the present study aims to analyze the formation of the 16

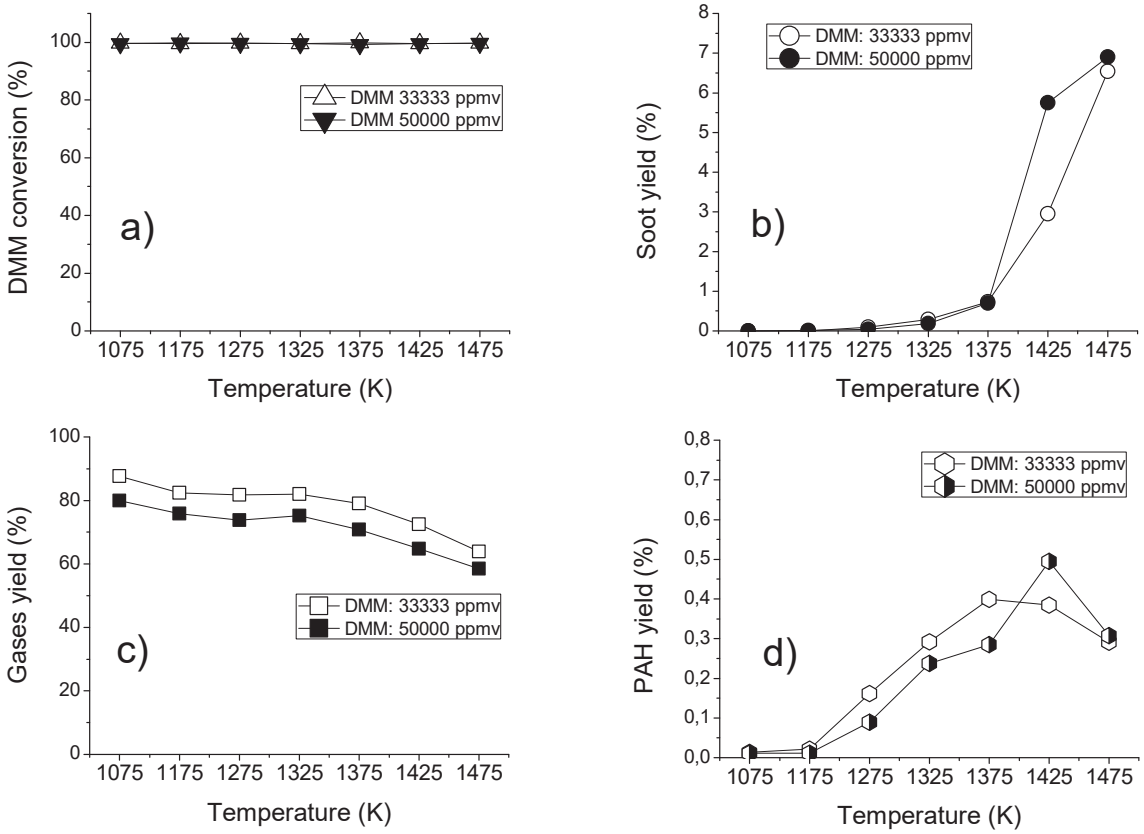

Fig. 2. Pyrolysis of DMM, for two inlet concentrations of fuel, as a function of the reaction temperature: a) conversion of DMM, b) yield to soot, c) yield to gases, and d) yield to PAH.

EPA-priority PAH during the pyrolysis of DMM by performing experiments in a tubular flow reactor installation operating at atmospheric pressure and with different reaction temperatures and inlet concentrations of DMM. The quantification of PAH present in different surfaces (soot and reactor walls) and at the outlet gas stream has been made to assess the distribution of PAH in each of these phases. Additionally, the toxicity of the PAH samples, expressed as B[*a*]P-eq, have been analyzed in all experiments. Finally, a comparison of the results obtained from this work with those obtained in previous works on the formation of soot and PAH during the pyrolysis of other oxygenated compounds is performed. Specifically, a comparison is carried out with alcohols (ethanol, butanol isomers: *iso*-butanol, 1-butanol, 2-butanol, *tert*-butanol), unsaturated cyclic ethers (2,5-dimethylfuran (2,5DMF), 2-methylfuran (2MF)), and a carbonate ester (dimethyl carbonate (DMC)). The results of this work contribute to the knowledge of the formation of PAH during the pyrolysis of DMM and associated toxicity, and help to figure out which type of fuel and operating conditions cause the least formation of these pollutants.

2. Experimental methodology

The experiments of the pyrolysis of DMM have been carried out in a facility with a flow reactor operating under well-established laboratory conditions. This installation has been used in several previous works of the group on the pyrolysis of oxygenated compounds e.g. [40,41]. The scheme of the installation can be found in Fig. 1.

Briefly, the reaction zone of the reactor, i.e., the heated isothermal region length, is of 160 mm, and is achieved by means of cooling air both at the exterior of the inlet and outlet of the reactor. In this work, the experimental conditions studied are similar to those used in the previous work of our research group on the pyrolysis of DMM [25], but in this case, the work in the present investigation is focused on the formation and quantification of the 16 EPA-priority PAH. The total gas flow was kept constant at 1000 mL (STP)/min, obtaining a gas residence time of 4168/T (K) (in seconds). The inlet concentrations of DMM were of 33,333 and 50,000 ppmv and were achieved through an isocratic HPLC bomb with an electric resistance to vaporize the liquid, while the temperatures in the reaction zone were 1075, 1175, 1275, 1325, 1375, 1425 and 1475 K. At the end of the reaction system, soot was collected by a quartz fiber cartridge (< 1 μm pore diameter), followed by a XAD-2 resin to collect PAH present in the gas-phase. Soot weight was calculated by the difference in mass of the cartridge before and after each experiment.

The sampling and analysis of PAH have been developed previously by our research group [42], according to EPA 3540C [43] and 8270D [44] methods and have been widely employed in previous studies [45,47]. A brief description of the procedure is shown below. PAH were analyzed in three phases: in the gas–phase, using the XAD-2 resin placed after the cartridge used to collect soot; on the reactor walls, by washing the reactor walls with 100 mL of dichloromethane; and on soot. The PAH adsorbed on the resin and soot were extracted by Soxhlet apparatus and concentrated using a rotary evaporator and a gentle stream of nitrogen.

The 16 EPA-priority PAH, were identified and quantified by a gas chromatograph (model 7890A) coupled to mass selective (model MSD 5975C) detector (GC–MS) of Agilent Technologies, with a capillary column DB-17Ms (60 m × 0.25 mm ID × 0.25 m). Selected ion monitoring (SIM) mode was employed to improve the selectivity and sensibility. The injection volume in splitless mode was 1 μL, with helium as carrier gas. The GC–MS was calibrated with a standard solution of the 16 priority PAH provided by Dr. Ehrenstorfer GmbH. The quantification method has shown recoveries greater than 80 % in several studies [38,40,45]. The method repeatability has been verified through the percent relative standard deviation (%RSD) of three trials, obtaining values lower than 22 % for most of the PAH [42]. The estimated uncertainty of the measurements is ± 5 %, but not less than 10 ppm, as eas

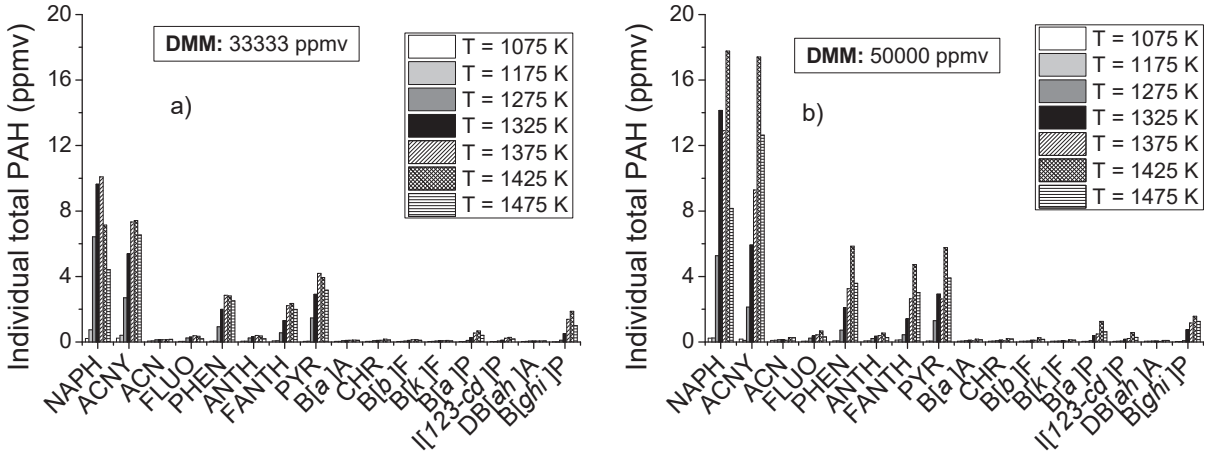

Fig. 3. Individual total PAH concentrations during the pyrolysis of DMM at different inlet concentrations of DMM and reaction temperatures.

reported in previous studies [38,40].

Besides, the B[*a*]P-eq (benzo[*a*]pyrene equivalent) was calculated to estimate the cancer risk attributed to the inhalation of PAH airborne samples Eq. (1). This value uses the toxicity equivalent factors (TEF) of each compound and its respective amount [PAH] in the sample [48,49].

$$B[a]P - eq = \sum_{i=1}^{n} (TEF_i) \times [PAH_i] \quad (1)$$

3. Results and discussion

3.1. Conversion of DMM

The conversion of DMM yields to soot, gases and PAH obtained in the pyrolysis of DMM, for two inlet concentrations of fuel (33,333 and 50,000 ppmv) as a function of the reaction temperature, is shown in Fig. 2. The yields are defined as the ratio, in percentage, between the carbon amount found in soot, outlet gases or PAH, respectively, and the carbon amount fed at the inlet of the reactor. The DMM conversion is high, over 95 %, for both concentrations of fuel tested, Fig. 2a. In general, by increasing the concentration of DMM, a higher yield to soot (Fig. 2b) and a lower yield to gases and PAH (Fig. 2c and 2d, respectively) are obtained. This is because as the higher the concentration of fuel is higher, the soot formation is enhanced and then, less carbon is available to participate in the formation of gases and PAH.

As expected, the yield to soot increases as the temperature increases (Fig. 2b), especially above 1375 K, reaching a value of around 7 % at the maximum temperature tested, for both inlet concentrations of DMM studied. On the other hand, the yield to gases decreases as the temperature increases (Fig. 2c) with values in the range of 63.8–87.6 % and 58.4–79.9 % for 33,333 and 50,000 ppmv, respectively. The yield to PAH (Fig. 2d) shows a maximum of around 0.5 % that coincides with a significant increase of soot formation (Fig. 2b), which indicates the consumption of PAH to form soot. These findings are consistent with those obtained in previous works on the pyrolysis of hydrocarbons and oxygenated compounds [38,39,45,46].

It is worth mentioning that DMM has a very low capacity to form soot and PAH because the carbon present in its structure is used to mainly form CO, thus removing carbon from the typical paths for the formation of soot and PAH, as will be discussed in more detail in section 3.4. Furthermore, the formation of small intermediated species, such as ethylene, acetylene, benzene, during the pyrolysis of DMM is low, as it has been reported early [25]. Ethylene can be formed through the $CH_3OCH_2OCH_3 \rightarrow CH_3OCHOCH_3 \rightarrow CH_3 \rightarrow C_2H_6 \rightarrow C_2H_5 \rightarrow C_2H_4$ reaction sequence. Then, ethylene can be converted to acetylene, with vinyl radicals (C_2H_3) as intermediate. Vinyl radicals subsequently are converted to vinylacetylene (C_4H_4) that can react with either vinyl radicals or with more acetylene to form benzene, and can also participate in PAH formation at higher temperatures [25].

3.2. PAH speciation

The individual total PAH speciation, which represents the sum of each concentration of analyte (PAH) found in XAD-2 resin, soot and reactor walls at each temperature tested during the pyrolysis of DMM, for two inlet concentrations of fuel (33,333 and 50,000 ppmv), as a function of the reaction temperature, is shown in Fig. 3.

The individual total PAH reaches a maximum value at intermediates temperatures, which can be attributed to their participation in the soot formation process. Moreover, for both inlet concentrations of DMM, the PAH with higher concentration are: NAPH, ACNY, PHEN, FANTH, PYR, and in minor amount the heavy ones, B[*a*]P and B[*ghi*]P. The same trend has also been observed in previous works on the pyrolysis of hydrocarbons and oxygenated compounds [38,39,45,47].

In order to explain the evolution of individual PAH, Figs. 4 and 5 show their speciation together with their distribution at the different phases (soot, resin and reactor walls), during the pyrolysis of DMM at 33,333 and 50,000 ppmv, respectively, and at all the temperatures studied.

For both inlet concentrations of DMM, the most predominant PAH are NAPH and ACNY, with a persistent presence in resin. While for NAPH this occurs at all temperatures and for both concentrations of fuel tested, for ACNY its highest concentration is shifted from resin to soot at 1375, 1425 and 1475 K. This behavior was also observed in a previous study on the pyrolysis of ethanol [38] and could be explained by the HACA route, that includes the addition of acetylene, from NAPH, up to the formation of ACNY at high temperatures [50].

At the highest temperatures, 1425–1475 K (Fig. 4f, 4 g, 5f and 5 g), it is observed a drastic increase in concentration of PAH in soot, especially of high molecular PAH, such as PHEN, FANTH, PYR, B[*a*]P and B[*ghi*]P. These results are in line with previous works [38,47], and could be because lighter PAH are generally in the gas-phase, while heavy PAH are in soot particles, mainly at high temperatures, where the soot formation process is favored [51].

3.3. PAH toxicity

The toxicity of the PAH samples, expressed as B[*a*]P-eq, from the pyrolysis of DMM with two inlet concentrations, 33,333 and 50,000 ppmv, as a function of the reaction temperature, is shown in Fig. 6. The toxicity presents a maximum at 1425 K in both cases that agree with the highest concentration of B[*a*]P in soot (Fig. 4f and 5f). Moreover, the

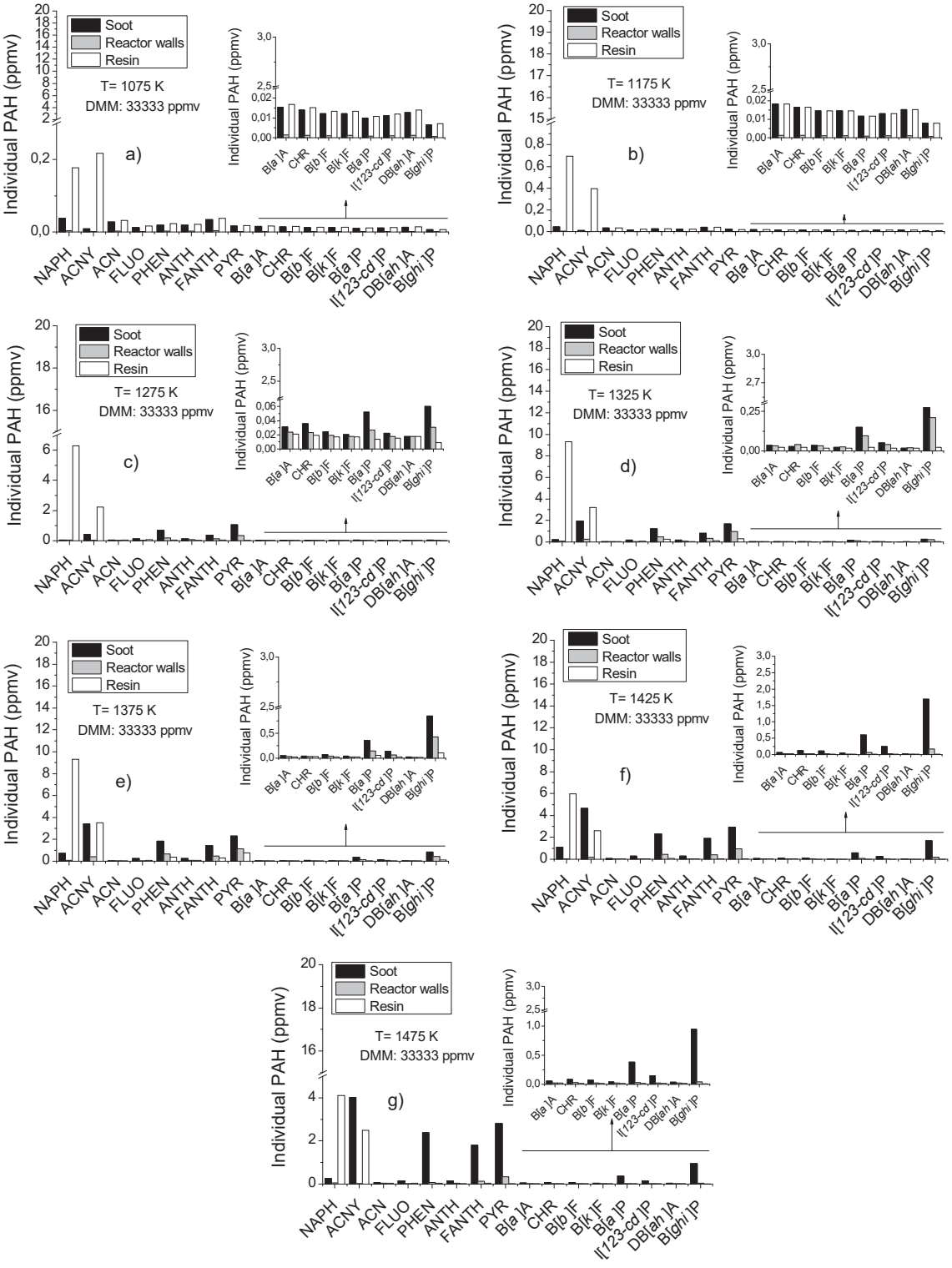

Fig. 4. Individual PAH distribution from the pyrolysis of DMM (33,333 ppmv) at different reaction temperatures: a) 1075 K, b) 1175 K, c) 1275 K, d) 1325 K, e) 1375 K, f) 1425 K, g) 1475 K.

higher the inlet concentration of DMM, the higher the toxicity.

The total PAH concentration and the toxicity in all phases studied (soot, reactor walls and resin) in the pyrolysis of DMM, for two inlet concentrations of DMM, as a function of the temperature is shown in Fig. 7.

Fig. 7 shows that total PAH are distributed principally in the resin up to 1375 K, while from 1425 K the distribution of total PAH is greater in soot, with the highest total concentration occurring at 1425 K. Regarding the toxicity, it is observed that it is higher on soot for any temperature studied and shows a maximum at the same temperature where a considerable increase in soot formation is produced (Fig. 2b). The maximum of total PAH concentration (Fig. 7) occurs at 1425 K, with a higher toxicity value during the pyrolysis of DMM 50000 ppmv (Fig. 7b). This indicates the adverse health effects of soot particles,

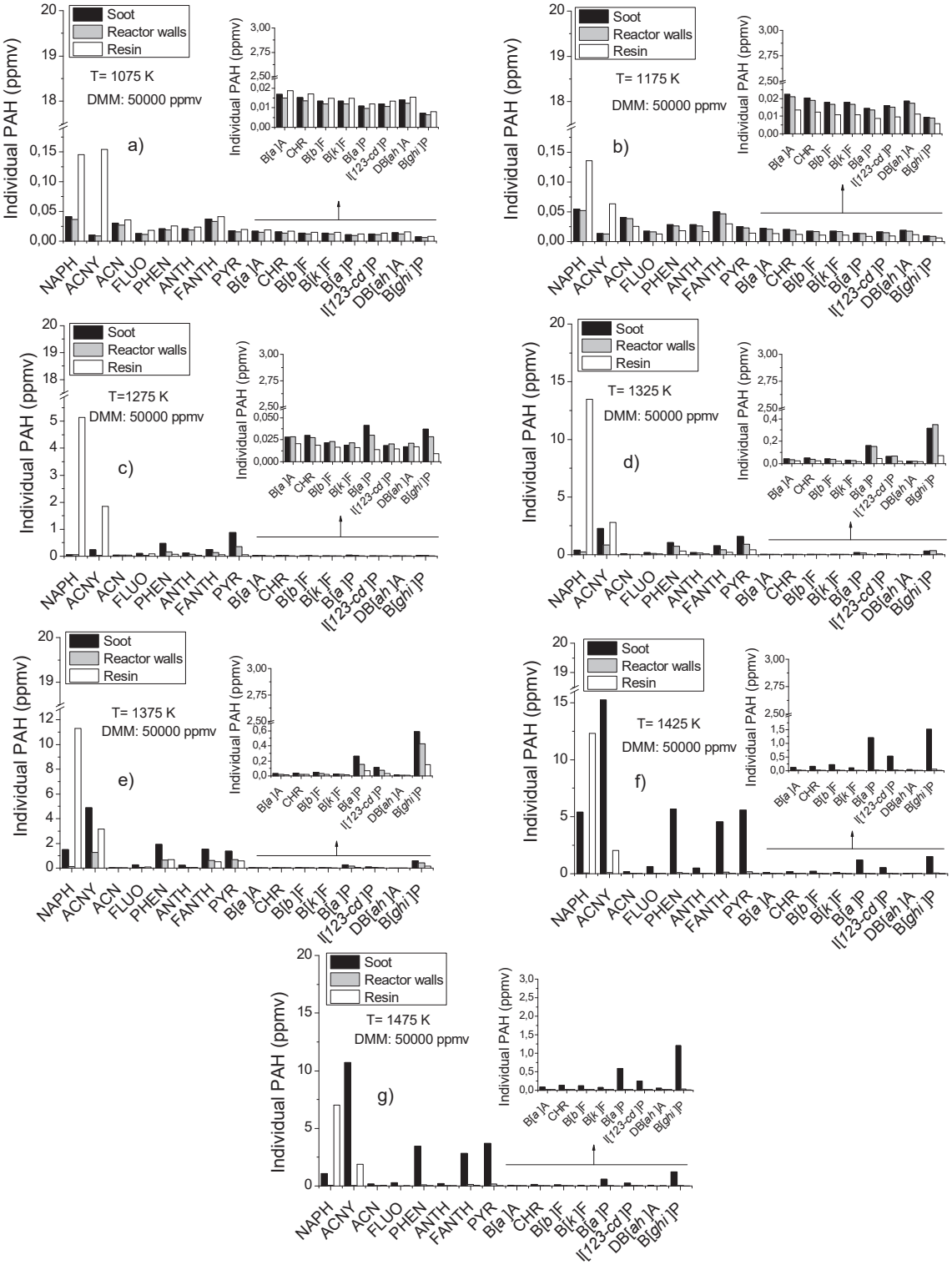

Fig. 5. Individual PAH distribution from the pyrolysis of DMM (50,000 ppmv) at different reaction temperatures: a) 1075 K, b) 1175 K, c) 1275 K, d) 1325 K, e) 1375 K, f) 1425 K, g) 1475 K.

which additionally to the effect produced by inhaling small size particles that exhibit high penetration in the respiratory system of humans, they also have associated a certain degree of toxicity.

3.4. Comparison of the pyrolysis of DMM and other oxygenated compounds

The importance of different oxygenated organic compounds analyzed as fuels or diesel additives, due to their potential for minimizing polluting emissions (soot, PAH), makes it interesting the comparison of the results obtained in the pyrolysis of these compounds. In

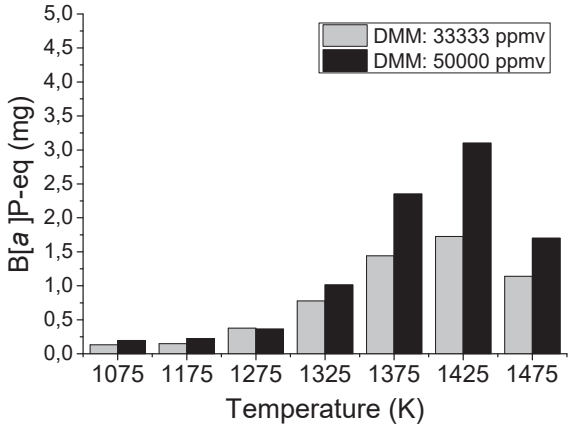

Fig. 6. B[*a*]P-eq values as a function of temperature, for two inlet concentrations of DMM.

this sense, this section shows a comparison of the results of the yield to products (soot, gases and PAH), PAH speciation, and PAH toxicity obtained both in this work and in previous pyrolysis experiments of different oxygenated compounds carried out in our group. The oxygenates compared cover a range of oxygen contents, types of chemical structures and functional groups, such as alcohols (ethanol, butanol isomers: 1-butanol, 2-butanol, *iso*-butanol and *tert*-butanol), unsaturated cyclic ethers (2,5-dimethylfuran (2,5DMF) and 2-methylfuran (2MF)), a carbonate ester (C(=O)OO) (dimethyl carbonate (DMC)) and an acyclic ether (O-C-O) (dimethoxymethane (DMM)), which are reported to be important factors controlling the sooting and PAH tendency of a fuel [52–57]. Literature results have shown clear effects of the presence of alcohols in alcohol-diesel fuel blends for PAH formation during diesel engines combustion e.g. [58,59].

For a proper comparison, the experimental conditions of the pyrolysis of each oxygenated compound were selected in order to be similar and are shown in Table 1. The comparison is performed for the temperatures of 1275, 1375 and 1475 K, a residence time (in seconds) of 4168/T (K) and an inlet concentration of carbon ranging from 90,000 to 150,000 ppm. It is worth mentioning that in the present work some additional experiments of the pyrolysis of 2,5DMF were carried out in order to have a complete overview of the PAH formed in the pyrolysis of furans, which chemical conversion has been analyzed in the past in our group.

Fig. 8 shows the comparison of the yield to soot, gases, and PAH for the reaction temperatures considered. In general, as the temperature increases, the yield to soot increases, while the yields to gases and PAH decrease. This is because the soot formation is favored at high temperatures, and carbon is being used in this process instead of being used to form gases or PAH. For all temperatures, *tert*-butanol, 2MF and 2,5DMF present the highest yield to soot, while DMC and DMM show the opposite (Fig. 8a). On the other hand, DMC and DMM have the highest yield to gases, at all temperatures tested, among all compounds compared (Fig. 8b). The fuel structure, functional group, as well as the routes involved in the formation of soot during the conversion of these species, have an important effect on its tendency to form the different products. In the case of *tert*-butanol, nine neighboring hydrogen atoms are available in the hydroxyl group to form complex bonds, and then an important pathway of fuel breaking of *tert*-butanol is through a complex fission to eliminate H_2O (R1) [47,61].

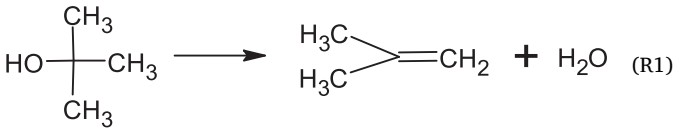

(R1)

It has also been identified that *tert*-butanol has high capacity to form C_3H_3 which, in turns, forms benzene and subsequently soot [62]. Regarding the cyclic species, also known as furans, (2,5DMF and 2MF), they have the ability to form soot through the conventional route (first break up into small fragments and then form the first ring, which is generally considered to be the rate-determining step in the soot formation process) and by a more direct pathway involving ring condensation or polymerization reactions building on the existing cyclic structure [54,63,64]. The consumption of 2,5DMF passes through cyclopentadienyl radicals (C_5H_5) up to formation of PAH rings (R2-R3).

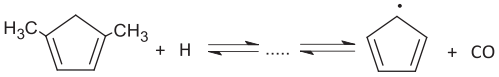

(R2)

(R3)

In the same way, the decomposition of 2MF conduces to the formation of vinyl radicals (C_2H_3) and vinyl acetylene (C_4H_4), which are involved in the formation of soot precursors such as benzene (R4-R7).

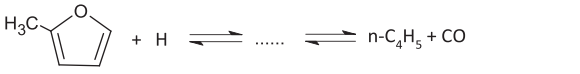

(R4)

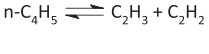

(R5)

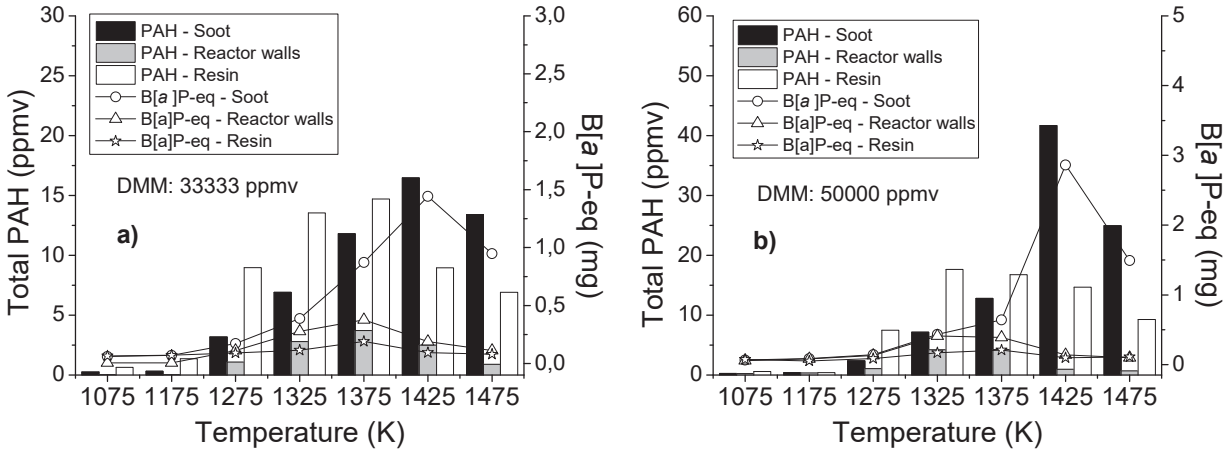

Fig. 7. Total PAH concentrations and B[*a*]P-eq values in all phases and at different temperatures tested, for both inlet concentrations of DMM: a) 33,333 ppmv, b) DMM 50,000 ppmv.

Table 1
Experimental conditions of the pyrolysis of the different oxygenated compounds.

Compound	Functional group	Chemical structure and formula	Inlet fuel concentration (ppmv)	Inlet carbon concentration (ppm)	Temperature (K)	Residencie time (s)	Reference
DMM	Acyclic ether	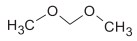 $C_3H_8O_2$	50,000	150,000	1275 1375 1475	$\frac{4168}{T(K)}$	Present work
Etanol	Alcohol	 C_2H_6O	50,000	100,000			[38]
1-butanol	Alcohol	 $C_4H_{10}O$	22,500	90,000			[47]
2-butanol	Alcohol	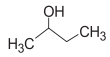 $C_4H_{10}O$	22,500	90,000			
Isobutanol	Alcohol	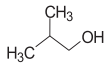 $C_4H_{10}O$	22,500	90,000			
Tert-butanol	Alcohol	 $C_4H_{10}O$	22,500	90,000			
2MF*	Unsaturated cyclic ether	 C_5H_6O	18,000	90,000			[60]
2,5DMF*		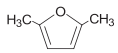 C_6H_8O	15,000	90,000			Present work
DMC	Carbonate ester	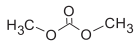 $C_3H_6O_3$	50,000	150,000			[40]

* Also known as furans.

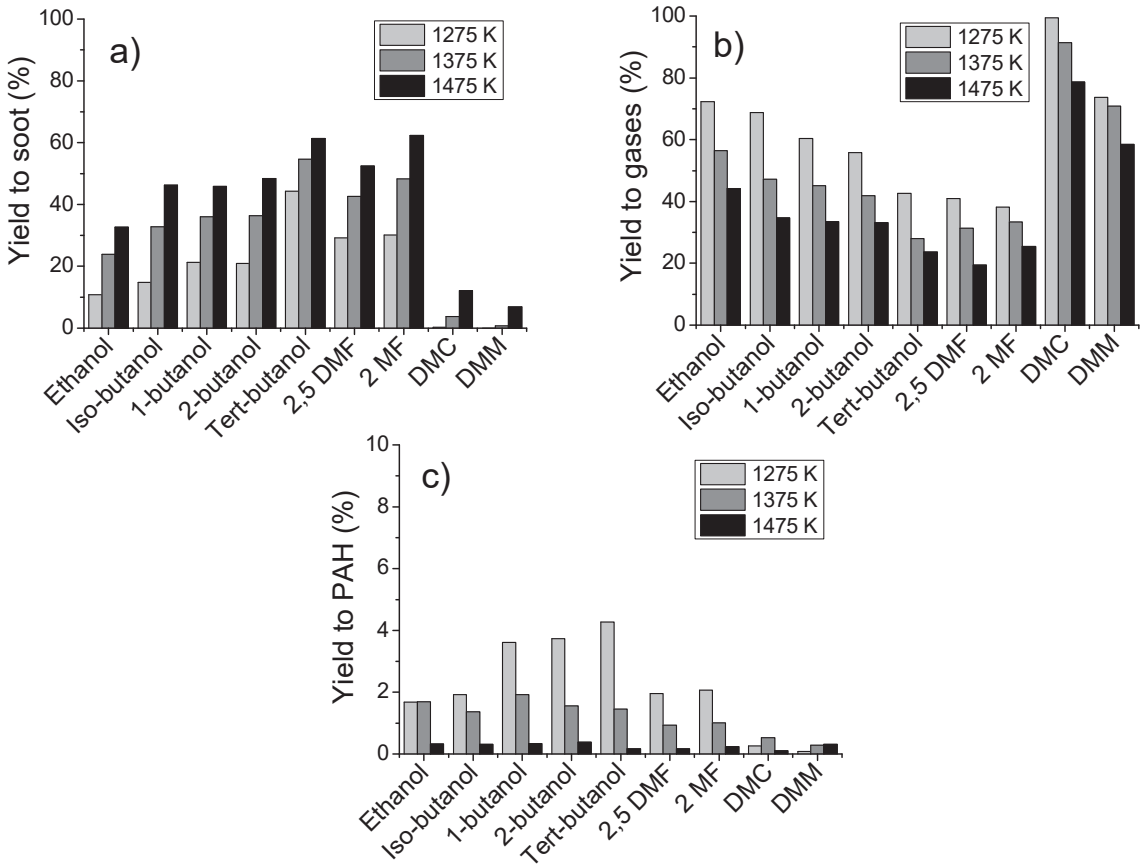

Fig. 8. Yield to products in the pyrolysis of different oxygenated organic compounds, for three reaction temperatures: 1275, 1375 and 1475 K. a) Yield to soot, b) Yield to gases, and c) Yield to PAH.

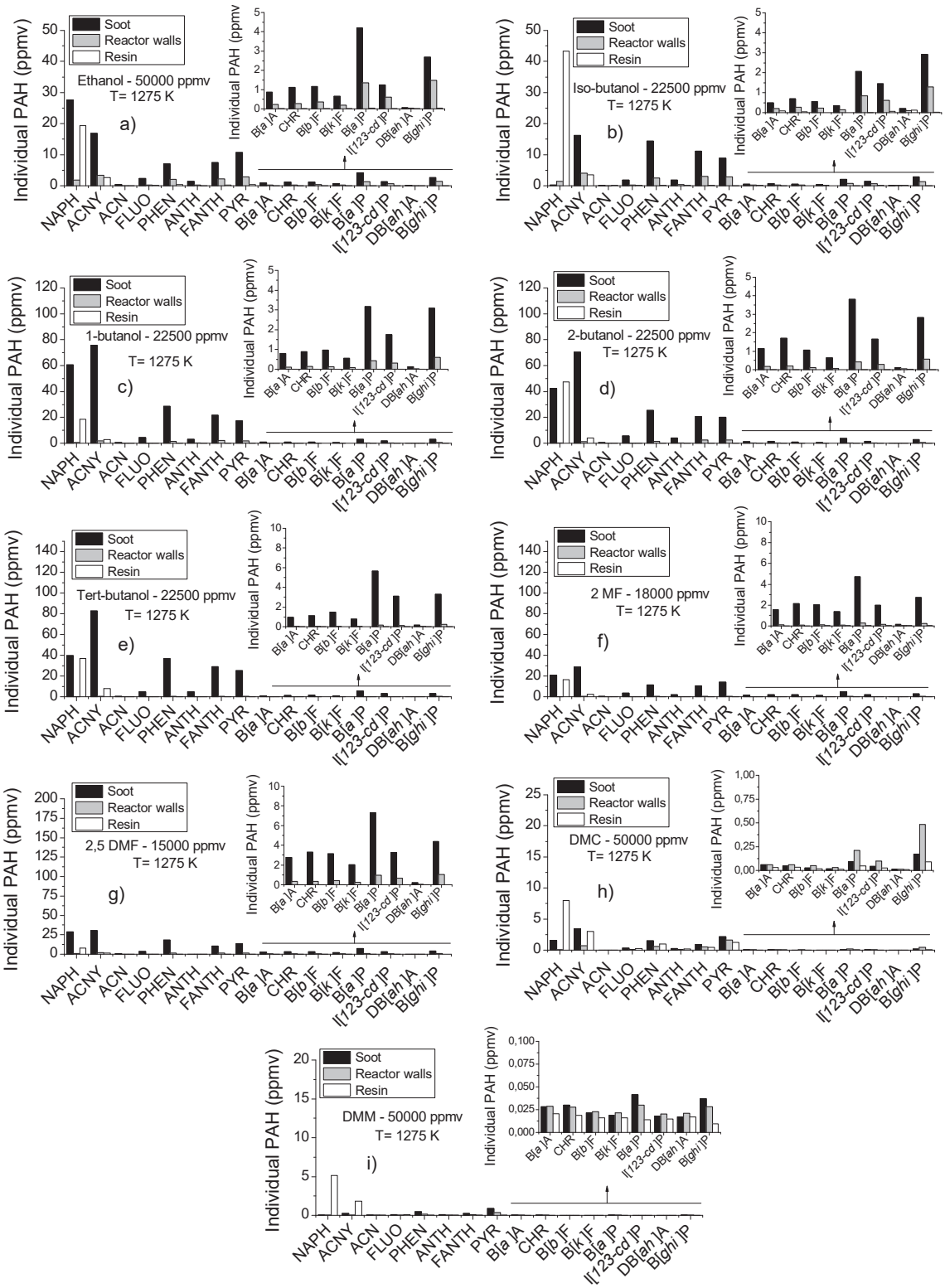

Fig. 9. Distribution of individual PAH from pyrolysis at 1275 K of: a) ethanol (50,000 ppmv), b) isobutanol (22,500 ppmv), c) 1-butanol (22,500 ppmv), d) 2-butanol (22,500 ppmv), e) *tert*-butanol (22,500 ppmv), f) 2MF (18,000 ppmv), g) 2,5DMF (15,000 ppmv), h) DMC (50,000 ppmv) and i) DMM (50,000 ppmv).

$$n\text{-}C_4H_5 \rightleftharpoons C_4H_4 + H \quad \text{(R6)}$$

$$C_4H_4 + C_2H_3 \rightleftharpoons \bigcirc + H \quad \text{(R7)}$$

The low tendency of DMC (carbonate ester) and DMM (acyclic ether) to form soot could be associated to the absence of C–C bonds in their molecular structure, which limits the capacity of these species to form soot precursors. It is interesting to note that, even though DMC has a higher oxygen content than DMM (53.3 wt% vs. 42.1 wt%), DMC has a higher capacity than DMM to form soot by a factor of around 1.7. Such

fact is mainly due to the specific molecular structure of these two oxygenates. In DMM, there are only C-O bonds in its structure and, during its pyrolysis, all O atoms in their molecular structure are being used to remove carbon from the typical paths that lead to the soot formation [25]. The decomposition of DMM leads to the formation of formaldehyde that conduces to the formation of CO and CO_2 (R8-R11).

(R8)

(R9)

(R10)

(R11)

Regarding DMC, the bond structure including O atoms leads to a considerable fraction of direct CO_2 formation, which wastes the oxygen in DMC [65]. Thus, DMC decomposes to methoxy formyl radicals and formaldehyde which in turn lead to the formation of CO and CO_2 (R12-R14).

(R12)

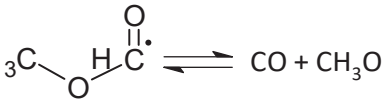

(R13)

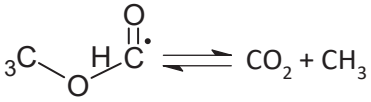

(R14)

On the other hand, for all temperatures, the yield to gases is greater in the pyrolysis of DMC and DMM and less for *tert*-butanol, 2MF and 2,5DMF (Fig. 8b). This is because carbon in DMC and DMM is used to form gas products, mainly CO and CO_2, instead soot (Fig. 8a) or PAH (Fig. 8c) [25,65]. Fig. 8c shows that, at 1475 K, the yield to PAH is less than 1 % for all oxygenated compounds, which could indicate that PAH formed during the pyrolysis of these compounds are converted, almost entirely, into soot. Furthermore, it is observed that at 1275 K the pyrolysis of all the oxygenates studied, except DMC and DMM, have a higher yield to PAH. This can be explained by the ease of leading to reaction pathways that favor the formation of PAH and subsequently its cyclization to form soot, which was explained above.

Fig. 9 shows the comparison of the PAH speciation at 1275 K, that is the temperature at which soot formation begins and the highest concentration of PAH is obtained in the pyrolysis of most of the compounds studied. The PAH obtained with the highest concentration in all the cases analyzed are: NAPH, ACNY, FLUO, PHEN, ANTH, FANTH and PYR, which represent more than 80 % of the PAH formed. Furthermore, the lowest PAH formation is observed in the pyrolysis of DMC and DMM. As mentioned above, the decomposition of these oxygenates mainly leads to the formation of gases such as CO and CO_2, removing carbon from the PAH and soot formation pathways.

Tran et al. [66] also observed increased formation of PAH, such as NAPH, PYR, and PHEN, during the study of 2,5DMF and 2MF in flame experiments. During the pyrolysis of alcohols, in a flow reactor, similar trend of the formation of NAPH was found [67], with the amount of the PAH formed in the pyrolysis of ethanol being lower than the obtained in the pyrolysis of 1-butanol and 2-butanol. Additionally, Chen et al. [62] showed, in flame experiments of diesel bends with butanol isomers, that the formation of PAH with 4 rings, such as PYR, would be directly related to the soot formation tendency. Similar results to those shown in the present work have been obtained in biomass pyrolysis studies [68], and in previous investigations of the pyrolysis of soot precursors, acetylene and ethylene, in which similar experimental conditions were used [39,45,46,69].

In general, PAH are mostly adsorbed on the surface of soot, except for NAPH, which can appear in significant concentrations both in the soot and the resin. It is also observed that in the pyrolysis of *tert*-butanol, 2MF and 2,5DMF, there is a higher concentration of high molecular weight PAH (Fig. 9e, 9f and 9g, respectively), which could condense and increase the formation of particles.

The total PAH concentrations and the toxicity in all phases studied (soot, reactor walls and resin) at 1275 K are shown in Fig. 10. The

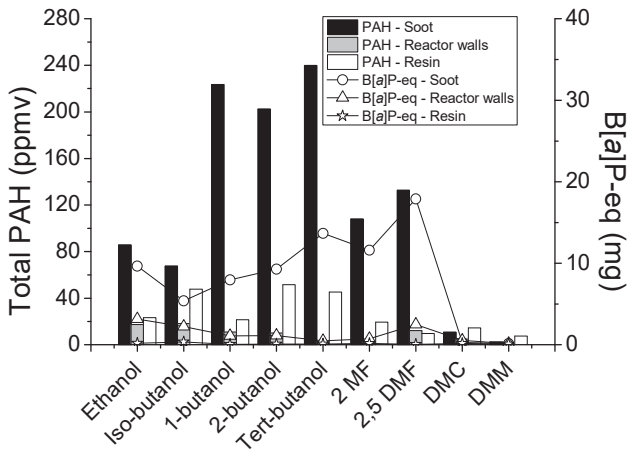

Fig. 10. Total PAH concentrations and B[*a*]P-eq values obtained in the pyrolysis of the oxygenated compounds, in the different phases analyzed (soot, reactor walls and resin) at 1275 K.

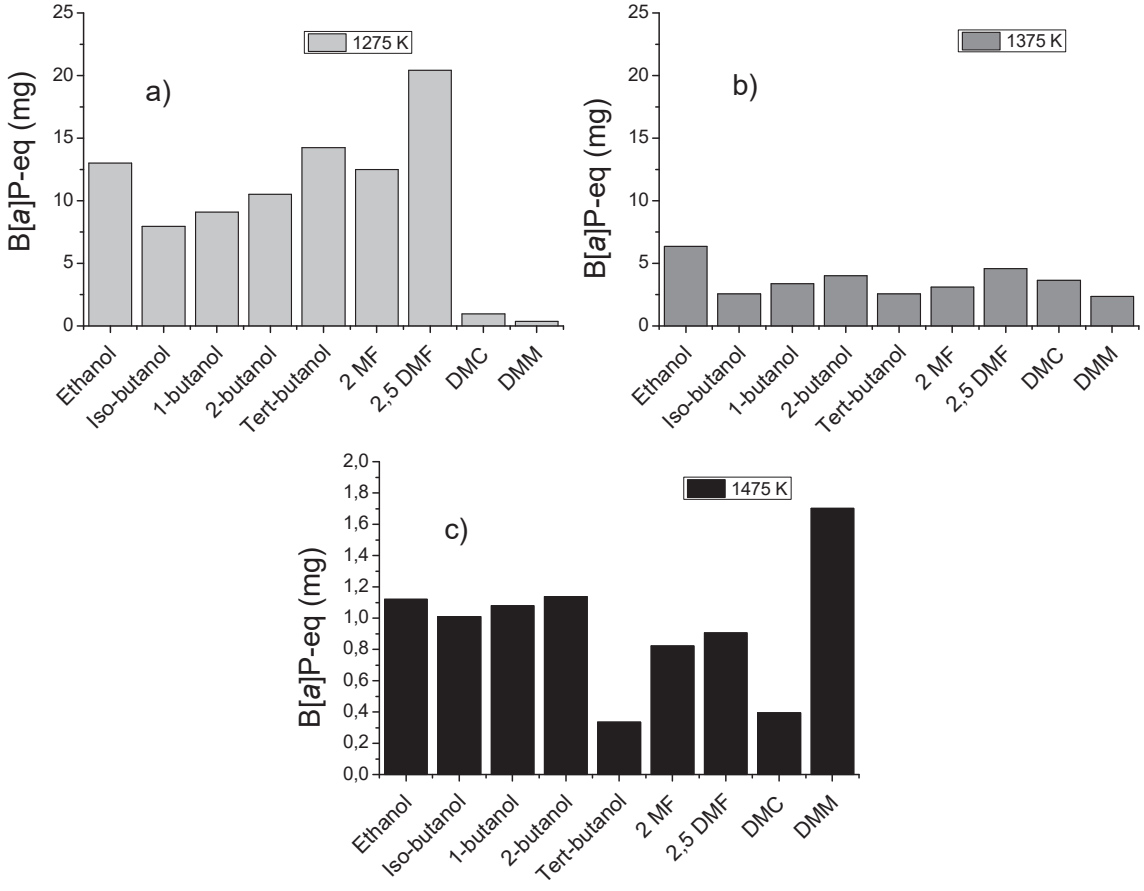

Fig. 11. B[*a*]P-eq values obtained during the pyrolysis of the oxygenated compounds at different temperatures: a) 1275 K, b) 1375 and c) 1475 K.

highest concentration of PAH is found adsorbed on soot and is obtained for 1-butanol, 2-butanol and *tert*-butanol. The highest B[*a*]P-eq value is also found in soot and occurs for *tert*-butanol, 2MF and 2,5DMF. These results could indicate that the pyrolysis of compounds with a branched or cyclic structure, with a greater number of C–C bonds, could present an effluent with a greater toxic risk in the initial stages of soot formation, since PAH with carcinogenic properties such as B[*a*]P would be adsorbed on the soot particles formed from the pyrolysis of these compounds.

The B[*a*]P-eq values obtained in the pyrolysis of the oxygenated compounds, considering all phases (soot, resin and reactor walls), at 1275, 1375 and 1475 K (Fig. 11) indicate that the highest B[*a*]P-eq value, for all the compounds, is found at the lowest temperature tested, except for DMM and DMC, due to their lowest PAH formation at this temperature, as it can be observed at Fig. 10. Moreover, at 1275 K, the highest toxicity is obtained in the pyrolysis of 2,5DMF, followed by the pyrolysis of alcohols, in particular by *tert*-butanol, Fig. 11a. This is in accordance with that observed in Fig. 9, which shows that the alcohols, 2MF and 2,5DMF give higher concentrations of B[*a*]P at 1275 K. At 1375 K (Fig. 11b), the toxicity decreases in the pyrolysis of all compounds except for DMC and DMM, which show a slight increase, while the pyrolysis of ethanol exhaust gases presents the greatest toxicity.

As mentioned, the toxicity was lower at 1475 K in all cases, compared to the other two temperatures studied (Fig. 11c) and it can be because the PAH with a greater number of rings formed during the pyrolysis, including B[*a*]P, become part of the soot particles [36]. The increased toxicity of DMM at high temperature is striking, since being a compound with a large proportion of oxygen (42 %), a behavior similar to the pyrolysis of DMC would be expected. In order to have an explanation of why the increase in toxicity for DMM occurs at the highest temperature studied, it would be necessary to carry out experiments at temperatures above 1475 K, the maximum temperature of the present work, in order to evaluate the trend as temperature is further increased.

4. Conclusions

The influence of the temperature and inlet concentration of fuel on the formation of the 16 EPA-priority PAH during the pyrolysis of dimethoxymethane (DMM) was analyzed, using inlet concentrations of fuel of 33,333 and 50,000 ppmv, and in the temperature range of 1075–1475 K. Additionally, a comparison with the results of the pyrolysis of different oxygenated compounds, focusing mainly on the formation of PAH was made.

Results indicate that the high yield to gases in the pyrolysis of DMM with a minimum value close to 60 %, for both concentrations of DMM tested, decreases the formation of soot and, consequently, the reduction of the yield to PAH, with values less than 0,5 %.

The yield to PAH presents a maximum, that could be due to the fact that PAH go from being a material formed by the breakdown of low-mass hydrocarbons, to becoming a precursor to the formation of soot via HACA route.

In the individual total PAH concentration, for both concentrations of DMM, the highest concentrations of PAH come from NAPH and ACNY, at all the temperatures tested, and are mostly distributed in the gas-phase (resin). The same trend is observed for the rest of oxygenated compounds analyzed.

The highest value of PAH toxicity is obtained comes from the pyrolysis of 50,000 ppmv of DMM, at 1425 K on soot, which could indicate that the higher the reaction temperature, the higher the toxicity of the

soot generated.

During the comparison of the pyrolysis of oxygenated compounds, the compounds that form higher soot amounts at 1475 K follow the trend: 2,5DMF < *tert*-butanol < 2MF < 2butanol < *iso*-butanol < 1-butanol < ethanol < DMC < DMM.

On the other hand, the trend to form PAH at 1275 K is *tert*-butanol < 2-butanol < 1-butanol < 2,5DMF < 2MF < *iso*-butanol < ethanol < DMC < DMM.

Considering the B[*a*]P-eq values, at 1275 K, the highest toxicity values come from 2,5DMF < *tert*-butanol < ethanol < 2 MF < 2-butanol < 1-butanol < *iso*-butanol < DMC < DMM.

Overall, DMM can be considered a good option for its use as a fuel additive due to its low ability to form soot and PAH under the conditions studied. However, further investigations under additional operating conditions, such as higher temperature and pressure, are needed to gain a more complete picture of the ability of DMM to form these pollutants.

CRediT authorship contribution statement

Fausto Viteri: Writing – review & editing, Writing – original draft, Visualization, Validation, Supervision, Methodology, Investigation, Formal analysis, Data curation, Conceptualization. **Katiuska Alexandrino:** Writing – review & editing, Writing – original draft, Methodology, Investigation. **Ángela Millera:** Writing – review & editing, Visualization, Conceptualization. **Rafael Bilbao:** Writing – review & editing, Resources, Conceptualization. **María U. Alzueta:** Writing – review & editing, Visualization, Supervision, Resources, Project administration, Funding acquisition, Conceptualization.

Declaration of competing interest

The authors declare that they have no known competing financial interests or personal relationships that could have appeared to influence the work reported in this paper.

Acknowledgements

The authors acknowledge to MINECO and FEDER (TED2021-129557B-I00 and PID2021-124032OB-I00) and the Aragón Government (ref. T22_23R), cofounded by FEDER 2014-2020 “Construyendo Europa desde Aragón”, for financial support. F. Viteri acknowledges the “Secretaría Nacional de Educación Superior, Ciencia, Tecnología e Innovación” (SENESCYT) for the predoctoral grant awarded.

Data availability

Data will be made available on request.

References

[1] Omari A, Heuser B, Pischinger S. Potential of oxymethylenether-diesel blends for ultra-low emission engines. Fuel 2017;209:232–7. https://doi.org/10.1016/j.fuel.2017.07.107.
[2] Ren Y, Huang Z, Miao H, Di Y, Jiang D, Zeng K, et al. Combustion and emissions of a DI diesel engine fuelled with diesel-oxygenate blends. Fuel 2008;87:2691–7. https://doi.org/10.1016/j.fuel.2008.02.017.
[3] Zhang C, Li P, Li Y, He J, Li X. Shock-tube study of dimethoxymethane ignition at high temperatures. Energy Fuels 2014;28:4603–10. https://doi.org/10.1021/ef500853v.
[4] Sathiyagnanam AP, Saravanan CG. Effects of diesel particulate trap and addition of di-methoxy-methane, di-methoxy-propane to diesel on emission characteristics of a diesel engine. Fuel 2008;87:2281–5. https://doi.org/10.1016/j.fuel.2007.12.003.
[5] Zhu R, Miao H, Wang X, Huang Z. Effects of fuel constituents and injection timing on combustion and emission characteristics of a compression-ignition engine fueled with diesel-DMM blends. Proc Combust Inst 2013;34:3013–20. https://doi.org/10.1016/j.proci.2012.06.174.
[6] Pan M, Qian W, Wang Y, Wu C, Huang H. Effect of dimethoxymethane (DMM) additive on combustion and emission characteristics under different working conditions in CI engines. Fuel 2021;284:119304. https://doi.org/10.1016/j.fuel.2020.119304.
[7] Zhang H, Kaczmarek D, Rudolph C, Schmitt S, Gaiser N, Oßwald P, et al. Dimethyl ether (DME) and dimethoxymethane (DMM) as reaction enhancers for methane: Combining flame experiments with model-assisted exploration of a polygeneration process. Combust Flame 2022;237:111863. https://doi.org/10.1016/j.combustflame.2021.111863.
[8] Shrestha KP, Eckart S, Drost S, Fritsche C, Schießl R, Seidel L, et al. A comprehensive kinetic modeling of oxymethylene ethers (OMEn, n=1–3) oxidation - Laminar flame speed and ignition delay time measurements. Combust Flame 2022;246:112426. https://doi.org/10.1016/j.combustflame.2022.112426.
[9] Gaiser N, Zhang H, Bierkandt T, Schmitt S, Zinsmeister J, Kathrotia T, et al. Investigation of the combustion chemistry in laminar, low-pressure oxymethylene ether flames (OME0-4). Combust Flame 2022;243:112060. https://doi.org/10.1016/j.combustflame.2022.112060.
[10] Shrestha KP, Eckart S, Elbaz AM, Gir BR, Fritsche C, Seidel L, et al. A comprehensive kinetic model for dimethyl ether and dimethoxymethane oxidation and NOx interaction utilizing experimental laminar flame speed measurements at elevated pressure and temperature. Combust Flame 2020;218:57–74. https://doi.org/10.1016/j.combustflame.2020.04.016.
[11] Daly CA, Simmie JM, Dagaut P, Cathonnet M. Oxidation of dimethoxymethane in a jet-stirred reactor. Combust Flame 2001;125:1106–17. https://doi.org/10.1016/S0010-2180(01)00227-9.
[12] Sun W, Tao T, Lailliau M, Hansen N, Yang B, Dagaut P. Exploration of the oxidation chemistry of dimethoxymethane: jet-stirred reactor experiments and kinetic modeling. Combust Flame 2018;193:491–501. https://doi.org/10.1016/j.combustflame.2018.04.008.
[13] Vermeire FH, Carstensen HH, Herbinet O, Battin-Leclerc F, Marin GB, Van Geem KM. Experimental and modeling study of the pyrolysis and combustion of dimethoxymethane. Combust Flame 2018;190:270–83. https://doi.org/10.1016/j.combustflame.2017.12.001.
[14] Wang H, Yao Z, Zhong X, Zuo Q, Zheng Z, Chen Y, et al. Experimental and kinetic modeling studies on low-temperature oxidation of Polyoxymethylene Dimethyl Ether (DMM1-3) in a jet-stirred reactor. Combust Flame 2022;245:112332. https://doi.org/10.1016/j.combustflame.2022.112332.
[15] Zhong X, Wang H, Zuo Q, Zheng Z, Wang J, Yin W, et al. Experimental and kinetic modeling studies of polyoxymethylene dimethyl ether (PODE) pyrolysis in jet stirred reactor. J Anal Appl Pyrolysis 2021;159:105332. https://doi.org/10.1016/j.jaap.2021.105332.
[16] Marrodán L, Royo E, Millera Á, Bilbao R, Alzueta MU. High pressure oxidation of dimethoxymethane. Energy Fuels 2015;29:3507–17. https://doi.org/10.1021/acs.energyfuels.5b00459.
[17] Marrodán L, Monge F, Millera Á, Bilbao R, Alzueta MU. Dimethoxymethane oxidation in a flow reactor. Combust Sci Technol 2016;188:719–29. https://doi.org/10.1080/00102202.2016.1138826.
[18] Zhang H, Schmitt S, Ruwe L, Kohse-Höinghaus K. Inhibiting and promoting effects of NO on dimethyl ether and dimethoxymethane oxidation in a plug-flow reactor. Combust Flame 2021;224:94–107. https://doi.org/10.1016/j.combustflame.2020.08.027.
[19] Jacobs S, Döntgen M, Alquaity ABS, Kopp WA, Kröger LC, Burke U, et al. Detailed kinetic modeling of dimethoxymethane. Part II: Experimental and theoretical study of the kinetics and reaction mechanism. Combust Flame 2019;205:522–33. https://doi.org/10.1016/j.combustflame.2018.12.026.
[20] Herzler J, Fikri M, Schulz C. High-pressure shock-tube study of the ignition and product formation of fuel-rich dimethoxymethane (DMM)/air and CH4/DMM/air mixtures. Combust Flame 2020;216:293–9. https://doi.org/10.1016/j.combustflame.2020.03.008.
[21] Peukert S, Sela P, Nativel D, Herzler J, Fikri M, Schulz C. Direct measurement of high-temperature rate constants of the thermal decomposition of dimethoxymethane, a shock tube and modeling study. J Phys Chem A 2018;122:7559–71. https://doi.org/10.1021/acs.jpca.8b06558.
[22] Golka L, Weber I, Olzmann M. Pyrolysis of dimethoxymethane and the reaction of dimethoxymethane with H atoms: A shock-tube/ARAS/TOF-MS and modeling study. Proc Combust Inst 2019;37:179–87. https://doi.org/10.1016/j.proci.2018.05.036.
[23] Li N, Sun W, Liu S, Qin X, Zhao Y, Wei Y, et al. A comprehensive experimental and kinetic modeling study of dimethoxymethane combustion. Combust Flame 2021;233:111583. https://doi.org/10.1016/j.combustflame.2021.111583.
[24] Drakon AV, Eremin AV, Zolotarenko VN, Korshunova MR, Mikheeva EY. Experimental investigation of the formation of polyaromatic hydrocarbons and soot during the pyrolysis of ethylene with the addition of dimethyl and diethyl ethers and dimethoxymethane. Combust Explos Shock Waves 2023;59:185–98. https://doi.org/10.1134/S0010508223020090.
[25] Alexandrino K, Millera Á, Bilbao R, Alzueta MU. Gas and soot formed in the dimethoxymethane pyrolysis. Soot characterization. Fuel Process Technol 2018;179:369–77. https://doi.org/10.1016/j.fuproc.2018.07.021.
[26] Lawal AT. Polycyclic aromatic hydrocarbons. A review. Cogent Environ Sci 2017;3:1339841. https://doi.org/10.1080/23311843.2017.1339841.
[27] United States Environmental Protection Agency (U.S. EPA). Health Assessment Document for Diesel Engine Exhaust; National Center for Environmental Assessment: Washington, D.C., 2002; Report EPA/600/8-90/057F. URL: https://cfpub.epa.gov/ncea/risk/recordisplay.cfm?deid=29060. Accessed: 10 June 2024.
[28] Albinet AE, Leoz Garziandia H, Budzinski E, Villenave JL. Jaffrezo, Nitrated and oxygenated derivatives of polycyclic aromatic hydrocarbons in the ambient air of two French alpine valleys part1: concentrations, sources and gas/particle partitioning. Atmos Environ 2008;42:43–54. https://doi.org/10.1016/j.atmosenv.2007.10.009.

[29] Huang B, Liu M, Bi X, Chaemfa C, Ren Z, Wang X, et al. Phase distribution, sources and risk assessment of PAH NPAH and OPAH in a rural site of Pearl River Delta region. China, Atmos Pollut Res 2014;5:210–8. https://doi.org/10.5094/APR.2014.026.

[30] Frenklach M, Wang H, Detailed Mechanism and Modeling of Soot Particle Formation. In Soot Formation in Combustion; Bockhorn, H., Eds.; Springer Series in Chemical Physics, Vol 59; Springer: Berlin,Heidelberg, 1994, p. 165-192. 10.1007/978-3-642-85167-4_10.

[31] Bohm H, Jander H. PAH formation in acetylene-benzene pyrolysis. Phys Chem Chem Phys 1999;1:3775–81. https://doi.org/10.1039/A903306H.

[32] Shukla B, Koshi M. A novel route for PAH growth in HACA based mechanisms. Combust Flame 2012;159:3589–96. https://doi.org/10.1016/j.combustflame.2012.08.007.

[33] Kislov KK, Islamova NI, Kolker AM, Lin SH, Mebel AM. Hydrogen abstraction acetylene addition and Diels-Alder mechanisms of PAH formation: a detailed study using first principles calculations. J Chem Theory Comput 2005;1:908–24. https://doi.org/10.1021/ct0500491.

[34] Harris SJ, Weiner AM. A picture of soot particle inception. Symp. Combust., [Proc.] 1989,;22:333-342. 10.1016/S0082-0784(89)80039-6.

[35] Kazakov A, Frenklach M. On the relative contribution of acetylene and aromatics to soot particle surface growth. Combust Flame 1998;112:270–4. https://doi.org/10.1016/S0010-2180(97)81776-2.

[36] Richter H, Howard JB. Formation of polycyclic aromatic hydrocarbons and their growth to soot: A review of chemical reaction pathways. Prog Energy Combust Sci 2000;26:565–608. https://doi.org/10.1016/S0360-1285(00)00009-5.

[37] Frenklach M. Reaction mechanism of soot formation in flames. Phys Chem Chem Phys 2002;4:2028–37. https://doi.org/10.1039/B110045A.

[38] Viteri F, López A, Millera Á, Bilbao R, Alzueta MU. Influence of temperature and gas residence time on the formation of polycyclic aromatic hydrocarbons (PAH) during the pyrolysis of ethanol. Fuel 2019;236:820–8. https://doi.org/10.1016/j.fuel.2018.09.061.

[39] Sánchez NE, Callejas A, Millera Á, Bilbao R, Alzueta MU. Polycyclic Aromatic Hydrocarbon (PAH) and soot formation in the pyrolysis of acetylene and ethylene: Effect of the reaction temperature. Energy Fuels 2012;26:4823–9. https://doi.org/10.1021/ef300749q.

[40] Viteri F, Salinas J, Millera Á, Bilbao R, Alzueta MU. Pyrolysis of dimethyl carbonate: PAH formation. J Anal Appl Pyrolysis 2016;122:524–30. https://doi.org/10.1016/j.jaap.2016.09.011.

[41] Alexandrino K, Salvo P, Millera Á, Bilbao R, Alzueta MU. Influence of the temperature and 2,5-dimethylfuran concentration on its sooting tendency. Combust Sci Technol 2016;188:651–66. https://doi.org/10.1080/00102202.2016.1138828.

[42] Sánchez NE, Salafranca J, Callejas A, Millera Á, Bilbao R, Alzueta MU. Quantification of polycyclic aromatic hydrocarbons (PAH) found in gas and particle phases from pyrolytic processes using gas chromatography–mass spectrometry (GC–MS). Fuel 2013;107:246–53. https://doi.org/10.1016/j.fuel.2013.01.065.

[43] United States Environmental Protection Agency (U.S. EPA). Soxhlet extraction, method 3540C. 1996. URL: https://www.epa.gov/sites/default/files/2015-12/documents/3540c.pdf. Accessed: Accessed: 05 apr 2024.

[44] United States Environmental Protection Agency (U.S. EPA). Determination of semivolatile organic compounds by Gas Chromatography/Mass Spectrometry (CG/MS), Method 8270D. 2007. URL: https://floridadep.gov/sites/default/files/EPA_8270D.pdf. Accessed: Accessed: 05 apr 2024.

[45] Sánchez NE, Callejas A, Millera Á, Bilbao R, Alzueta MU. Formation of PAH and soot during acetylene pyrolysis at different gas residence times and reaction temperatures. Energy 2012;43:30–6. https://doi.org/10.1016/j.energy.2011.12.009.

[46] Sánchez NE, Callejas A, Millera Á, Bilbao R, Alzueta MU. Influence of the oxygen presence on polycyclic aromatic hydrocarbon (PAH) formation from acetylene pyrolysis under sooting conditions. Energy Fuels 2013;27:7081–8. https://doi.org/10.1021/ef401484s.

[47] Viteri F, Gracia S, Millera Á, Bilbao R, Alzueta MU. Polycyclic aromatic hydrocarbons (PAH) and soot formation in the pyrolysis of the butanol isomers. Fuel 2017;197:348–58. https://doi.org/10.1016/j.fuel.2017.02.026.

[48] Sauvain JJ, Vu Duc T, Guillemin M. Exposure to carcinogenic polycyclic aromatic compounds and health risk assessment for diesel-exhaust exposed workers. Int Arch Occup Environ Health 2003;76:443–55. https://doi.org/10.1007/s00420-003-0439-4.

[49] Nisbet ICT, LaGoy PK. Toxic equivalency factors (TEFs) for polycyclic aromatic hydrocarbons (PAH). Regul Toxicol Pharm 1992;16:290–300. https://doi.org/10.1016/0273-2300(92)90009-X.

[50] Richter H, Mazyar OA, Sumathi R, Green WH, Howard JB, Bozzelli JW. Detailed kinetic study of the growth of small polycyclic aromatic hydrocarbons. 1. 1-Naphthyl+ Ethyne. J Phys Chem A 2001;105:1561-73. 10.1021/jp002428q.

[51] Hytönen K, Yli-Pirilä P, Tissari J, Gröhn A, Riipinen I, Lehtinen KEJ, et al. Gas–particle distribution of PAH in wood combustion emission determined with annular denuders, filter, and polyurethane foam adsorbent. Aerosol Sci Technol 2009;43:442–54. https://doi.org/10.1080/02786820802716743.

[52] Barrientos EJ, Lapuerta M, Boehman AL. Group additivity in soot formation for the example of C-5 oxygenated hydrocarbons fuels. Combust Flame 2013;160:1484–98. https://doi.org/10.1016/j.combustflame.2013.02.024.

[53] Esarte C, Millera A, Bilbao R, Alzueta MU. Effect of ethanol, dimethylether, and oxygen, when mixed with acetylene, on the formation of soot and gas products. Ind Eng Chem Res 2010;49:6772–9. https://doi.org/10.1021/ie901663g.

[54] Ladommatos N, Rubenstein P, Bennett P. Some effects of molecular structure of single hydrocarbons on sooting tendency. Fuel 1996;75:114–24. https://doi.org/10.1016/0016-2361(94)00251-7.

[55] Lemaire R, Lapalme D, Seers P. Analysis of the sooting propensity of C-4 and C-5 oxygenates: comparison of sooting indexes issued from laser-based experiments and group additivity approaches. Combust Flame 2015;162:3140–55. https://doi.org/10.1016/j.combustflame.2015.03.018.

[56] McEnally CS, Pfefferle LD. Improved sooting tendency measurements for aromatic hydrocarbons and their implications for naphthalene formation pathways. Combust Flame 2007;148:210–22. https://doi.org/10.1016/j.combustflame.2006.11.003.

[57] McEnally CS, Pfefferle LD. Sooting tendencies of oxygenated hydrocarbons in laboratory-scale flames. Environ Sci Technol 2011;45:2498–503. https://doi.org/10.1021/es103733q.

[58] Yilmaz N, Vigil F, Donaldson B. Effect of n-butanol addition to diesel fuel on reduction of PAH formation and regulated pollutants. Polycycl Aromat Comp 2002;43:8785–99. https://doi.org/10.1080/10406638.2022.2153881.

[59] Yilmaz N, Atmanli A, Vigil FM, Donaldson B. Comparative assessment of polycyclic aromatic hydrocarbons and toxicity in a diesel engine powered by diesel and biodiesel blends with high concentrations of alcohols. Energies 2022;15:8523. https://doi.org/10.3390/en15228523.

[60] Viteri F, Baena C, Millera Á, Bilbao R, Alzueta MU. Formation of polycyclic aromatic hydrocarbons in the pyrolysis of 2-methylfuran at different reaction temperatures. Combust Sci Technol 2016;188:611–22. https://doi.org/10.1080/00102202.2016.1138827.

[61] Singh P, Hui X, Sung CJ. Soot formation in non-premixed counterflow flames of butane and butanol isomers. Combust Flame 2016;164:167–82. https://doi.org/10.1016/j.combustflame.2015.11.015.

[62] Chen B, Liu X, Liu H, Wang H, Kyritsis DC, Yao M. Soot reduction effects of the addition of four butanol isomers on partially premixed flames of diesel surrogates. Combust Flame 2017;177:123–36. https://doi.org/10.1016/j.combustflame.2016.12.012.

[63] Agafonov GL, Smirnov VN, Vlasov PA. Shock tube and modeling study of soot formation during the pyrolysis and oxidation of a number of aliphatic and aromatic hydrocarbons. Proc Combust Inst 2011;33:625–32. https://doi.org/10.1016/j.proci.2010.07.089.

[64] Graham SC, Homer JB, Rosenfeld JLJ. The formation and coagulation of soot aerosols generated by the pyrolysis of aromatic hydrocarbons. Proc R Soc London, Ser A 1975;344:259–85. http://www.jstor.org/stable/78961.

[65] Alexandrino K, Salinas J, Millera Á, Bilbao R, Alzueta MU. Sooting propensity of dimethyl carbonate, soot reactivity and characterization. Fuel 2016;183:64–72. https://doi.org/10.1016/j.fuel.2016.06.058.

[66] Tran LS, Sirjean B, Glaude P, Kohse-Höinghaus K, Battin-Leclerc F. Influence of substituted furans on the formation of polycyclic aromatic hydrocarbons in flames. Proc Combust Inst 2015;35:1735–43. https://doi.org/10.1016/j.proci.2014.06.137.

[67] Khan ZZ, Hellier P, Ladommatos N. Measurement of soot mass and PAH during the pyrolysis of C2–C4 alcohols at high temperatures. Combust Flame 2022;236:111803. https://doi.org/10.1016/j.combustflame.2021.111803.

[68] McGrath T, Sharma R, Hajaligol M. An experimental investigation into the formation of polycyclic-aromatic hydrocarbons (PAH) from pyrolysis of biomass materials. Fuel 2001;80:1781–97. https://doi.org/10.1016/S0016-2361(01)00062-X.

[69] Sánchez NE, Millera Á, Bilbao R, Alzueta MU. Polycyclic aromatic hydrocarbons (PAH), soot and light gases formed in the pyrolysis of acetylene at different temperatures: Effect of fuel concentration. J Anal Appl Pyrolysis 2013;103:126–33. https://doi.org/10.1016/j.jaap.2012.10.027.